

1 1. **QUIC model simulation theory**

2 Quick Urban & Industrial Complex (QUIC) Dispersion Modeling System rapidly enables rapid
3 and detailed modeling of flow field around buildings and apply this generated wind profile in a
4 particle dispersion model. In the simulation, emissions from 250 sources are tracked
5 simultaneously to quantify the pollution concentration in the selected region. The QUIC model
6 stands out due to its ability to capture turbulence and the effect on pollution dispersion in the
7 vicinity of buildings. The model also provides building-scale results that can show emission hot
8 spots and concentrations and their interaction to eddies and current in the built environment. This
9 is achieved by combining mathematical models QUIC-URB and QUIC-PLUME. QUIC-URB
10 simulates the velocity wind field with building obstacles and QUIC-PLUME is a Lagrangian
11 random-walk particle dispersion model, which calculates pollution concentration distribution in
12 the field, the theory of each model is described below:

13 QUIC – URB is a diagnostic wind solver that computes the flow of 3D wind fields around the
14 buildings. The model is based on the algorithm first developed by Röckle et al. (Röckle, 1990). In
15 this fast response urban wind model, the initial velocity fields (u_o, v_o, w_o) are determined based on
16 empirical parameterizations such as upwind and downwind cavities, street canyons and
17 recirculation zones. After assigning initial velocity, the wind field is adjusted to satisfy mass
18 conservation equation (Singh et al., 2008; 磯部, 2013).

19 QUIC-URB algorithm considers empirical wind parameterizations, which is capable of simulating
20 eddies introduced to the building wake, thus providing complex turbulent flow fields. The street
21 canyon (SC) algorithm is applied for simulating flows in building wakes (Singh et al., 2008). SC
22 assumes that canyon flow could be categorized to skimming and isolated flow. When buildings
23 are widely spaced, the flow pattern is similar to flow around two isolated buildings, which is
24 denoted as isolated regime. As the distance between the building reduces, the building downstream
25 obstructs the wake produced by the upwind building until the initial flow starts skimming over the
26 buildings and drives eddies in the cavity, thus produces a strong vortex between these two
27 structures, this is defined as the skimming regime.

28 Skimming regime is applied when:

$$29 \quad \frac{s}{H} < 1.25 + 0.15 \frac{W}{H} \text{ when } \frac{W}{H} < 2, \text{ or}$$

$$30 \quad \frac{S}{H} < 1.55 \text{ when } \frac{W}{H} > 2$$

31 Isolated regime is applied when:

$$32 \quad \frac{S}{H} > 1.25 + 0.15 \frac{W}{H}$$

33 Where S is the building spacing, H is the building height and W is the building width.

34 The formulation for specification of the initial velocity field between the buildings is:

$$35 \frac{u_0}{U(H)} = -\frac{d}{0.5S} \left(\frac{S-d}{0.5S} \right)$$

$$36 \frac{w_0}{U(H)} = -\frac{1}{2} \left(1 - \frac{d}{0.5S} \right) \left(1 - \frac{S-d}{0.5S} \right)$$

37 Where d is the distance downwind from the upwind building, w is the vertical velocity component,
38 U(H) is the wind velocity at the top of the upwind building.

39 The mean wind field at height(z) above the building is calculated based on:

$$40 u(z) = \frac{u_*}{k} \ln \left(\frac{z}{z_0} \right)$$

41 Where, u_* = friction velocity, z_0 = aerodynamic roughness.

42

43 The QUIC-PLUME model is a Lagrangian random-walk model, wherein the movement of gases
44 and aerosols are tracked as they disperse in the air. The model deploys mean wind fields produced
45 by QUIC-URB model. The presence of buildings causes horizontal inhomogeneity of the flow.
46 The model applies a non-local mixing formulation that better quantifies the building wakes and
47 cavities in street canyon. The algorithm uses the mean motions from QUIC-URB output and
48 computes the horizontal gradients in turbulence parameters using the Langevin random walk
49 equations(Williams et al., 2004).

50 Lagrangian random-walk model describe dispersion of airborne contaminants by tracking the
51 release of air parcels and moving them with instantaneous wind, which is the combination of mean
52 wind and turbulent wind(Michael D. Williams, Michael J. Brown, 2005). The equation describes
53 the parcel position are:

$$54 x = x_p + U\Delta t + \frac{u'_p + u'}{2} \Delta t,$$

$$55 y = y_p + V\Delta t + \frac{v'_p + v'}{2} \Delta t,$$

$$56 z = z_p + W\Delta t + \frac{w'_p + w'}{2} \Delta t,$$

57 Where x,y and z are longitudinal, lateral, and vertical position coordinates of the particle, U ,V ,
58 and W are the x, y, and z components of the mean wind, u' , v' , and w' are the turbulent
59 components of the instantaneous wind, and Δt is the time step.

60 The fluctuating components of the wind are calculated from:

61 $u'(t + \Delta t) = u'(t) + du,$

62 $v'(t + \Delta t) = v'(t) + dv,$

63 $w'(t + \Delta t) = w'(t) + dw,$

64 The details of set of equations to derive du , dv and dw from Folker-Planck equations and well-
 65 mixed condition can be found in the QUIC-PLUME theory guide(Williams et al., 2004).The local
 66 coordinate system, the treatment of non-local mixing, and reflection are described. The pollution
 67 concentration in unit release is estimated by equation:

68
$$x_{i,j,k} = \frac{Q\Delta t_c}{n_{tot}d_{xb}d_{yb}d_{zb}t_{ave}}$$

69 This is the sum of PM2.5 particles that are found in the sampling domain during the average time
 70 t_{ave} , n_{tot} is the total number of particles released, d_{xb} , d_{yb} , and d_{zb} are the dimensions of the sampling
 71 domain, and Δt_c is the particle time step.

72 All scenarios were simulated under similar meteorological and environmental conditions. The
 73 QUIC model is used to simulate local pollution concentrations from continuously released
 74 emission sources over the average cooking period. Concentration data in each receptor grid were
 75 then extracted and processed by MATLAB.

76 2. Validation of QUIC model (water channel experiment)

77 The building wake was reproduced using Lego™ built block in a re-circulating water channel with
 78 honeycomb baffles to create laminar flow fields. The water tank geometry is shown in S5, and the
 79 experiment setup schematic is demonstrated in S6. The channel has flow control capability to
 80 maintain constant velocity for creating steady state. Fluorescent dye was released from a tube on
 81 top of the upwind building to simulate the stack emission through chimney. Videos of the dye
 82 release are recorded and divided into sequential photos to visualize the flow field in the building
 83 wake and to quantify pollution dispersion proportional to dye concentration, which are averaged
 84 to quantify pollution concentrations under steady state flow. The mocked-building wake water
 85 tank experiment is based on the following theory:

86 For an incompressible Newtonian fluid, the mass conservation and Navier-Stokes(momentum)
 87 equations of motion can be expressed as:

88
$$\frac{\alpha \bar{u}_i}{\alpha x_i} = 0$$

89
$$\frac{\alpha u_i}{\alpha t} + u_j \frac{\alpha u_i}{\alpha x_j} = f_i - \frac{1}{\rho} \frac{\alpha p}{\alpha x_i} + \nu \frac{\alpha^2 u_i}{\alpha x_j \alpha x_j}$$

90

91 Now, the scaling parameter is introduced to non-dimensionalize the Navier-Stokes equations. The
 92 technique can reduce the number of free parameters.

scale	Dimensionless variable
Length L	$x^*=x/L$
Flow velocity U	$u^*=u/U$
Time L/U	$t^*=t/(L/U)$
Pressure P	$p^*=P/(\rho U^2)$

93

94
$$\frac{\alpha u^*}{\alpha t^*} + u^* \frac{\alpha u^*}{\alpha x^*} = -\frac{\alpha P^*}{\alpha x^*} + \frac{1}{Re} \frac{\alpha^2 u^*}{\alpha x^{*2}} + \frac{1}{Fr^2} g$$

95 When the flow in the water channel is turbulent enough ($Re > 5000$), the term $\frac{\alpha \bar{u}_i}{\alpha x_j}$ is negligible and
 96 thus, the viscosity is neglected, this is fluid property; the Reynolds stress and turbulent stress
 97 dominant the flow, which are flow property instead of fluid properties. Thus, the water can imitate
 98 the flow in the atmosphere environment under turbulent conditions.

99 A dimensionless length scale factor ϕL is defined as

100

101

102
$$\phi L = \frac{[L]_{field}}{[L]_{lab}}$$

103

104 where L is the length scale.

105 The dimensionless time scale factor ϕT is defined as

106

107
$$\phi L = \frac{[t]_{field}}{[t]_{lab}} = \frac{\frac{L}{[U]_{field}}}{\frac{L}{[U]_{lab}}} = \frac{[L]_{field} [U]_{lab}}{[L]_{lab} [U]_{field}} = \frac{\phi L}{\phi U}$$

108

109 where U is the velocity of ambient flow, ϕU is a velocity scale factor.

110 The ambient concentration C for well mixed contaminant can be expressed as:

111

$$C = \frac{Q \times t}{V}$$

112

113

114 Where Q is the source mass flow rate, mg/s, t is the travel time of the contaminant; V is the control
115 volume.

116 The concentration scale factor is introduced as:

117

$$\varphi C = \frac{[C]_{field}}{[C]_{lab}} = \frac{\left[\frac{Q \times t}{V}\right]_{field}}{\left[\frac{Q \times t}{V}\right]_{lab}} = \frac{\left[\frac{Q \times t}{L^3}\right]_{field}}{\left[\frac{Q \times t}{L^3}\right]_{lab}} = \frac{[Q]_{field} \varphi C}{[Q]_{lab} \varphi L^3}$$

118

119

120 which can be rewritten as:

121

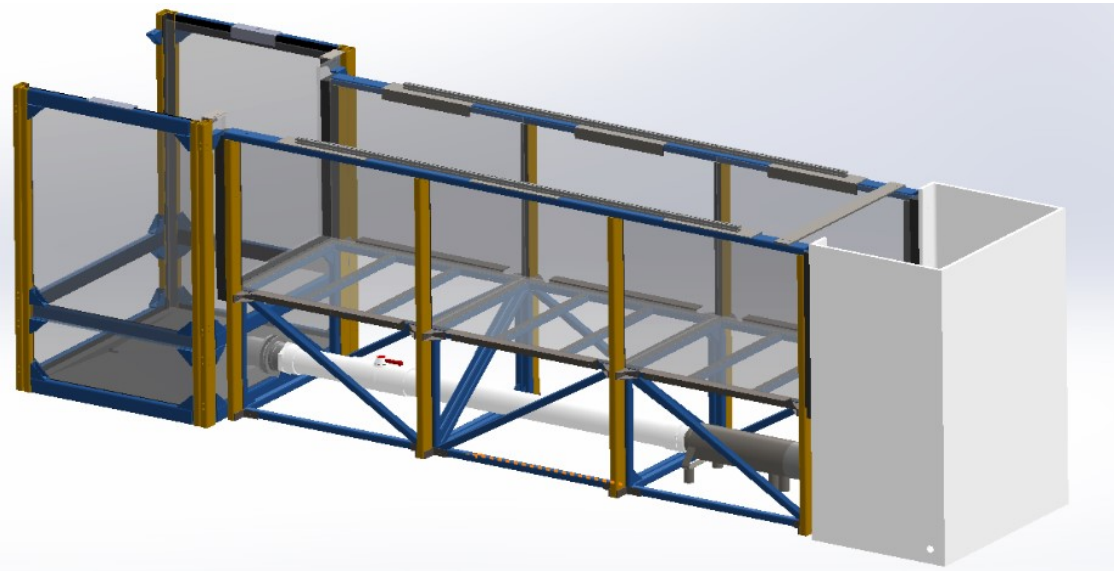
$$\varphi C = \frac{[C]_{field}}{[C]_{lab}} = \frac{[Q]_{field} [UL^2]_{lab}}{[Q]_{lab} [UL^2]_{field}}$$

122

123 The flow velocity in lab (U_{lab}) is 0.04 m/s. The height of the building H_{lab} is 10 cm. and distance
124 between the buildings is 20 cm. The volumetric flow rate of releasing the dye is $3.3 \times 10^{-6} \text{ m}^3$. The
125 experiment was recorded by camera, and the image was post processed to get the relative
126 concentration.

127

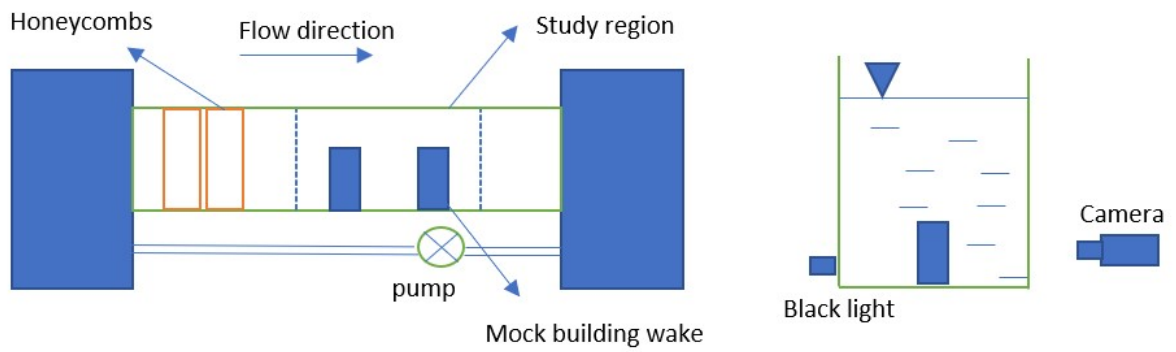
128



129

130

Figure S1. Water tank geometry



131

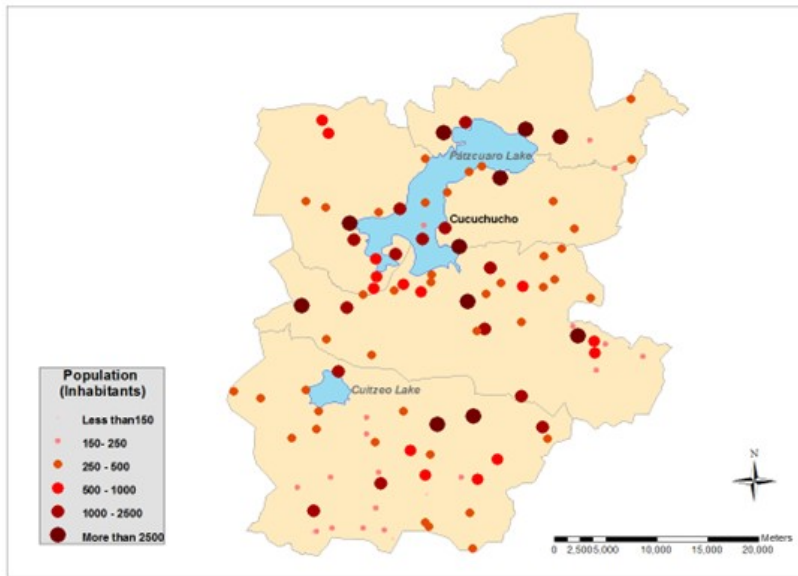
132

133

Figure S2. Experiment setup schematic

134

135 **3. Geophysical information**

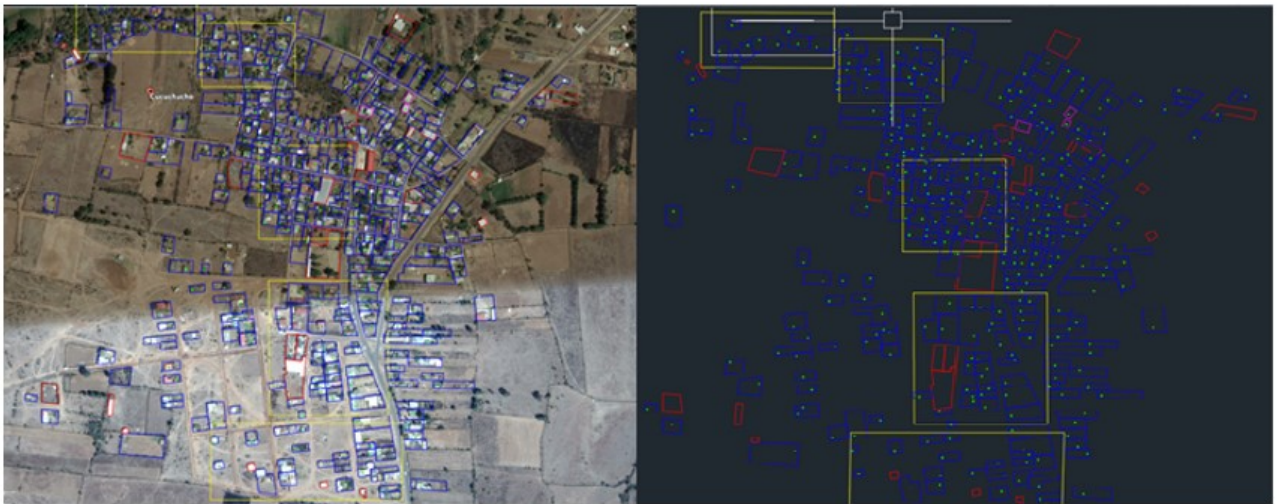


136

137 Figure S3. Local inhabitants' distribution near the selected region

a)

b)



138

139 Figure S4. a) Distribution of households in the village

140 b) Distribution of emission sources on rooftop of households (represented by white dot)

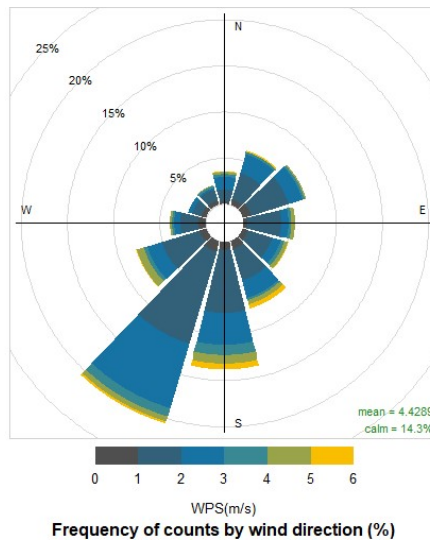
141

142

143

144

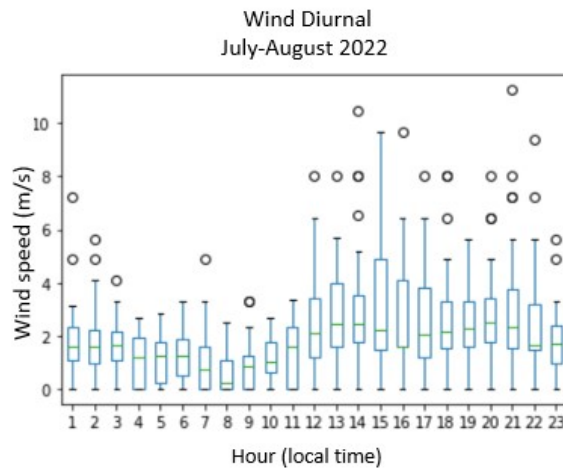
4. Meteorology information



145

146

Figure S5. Wind rose for July-August near Cucuchucho



147

148

Figure S6. Wind diurnal for July-August

149

150

151

152

153

154

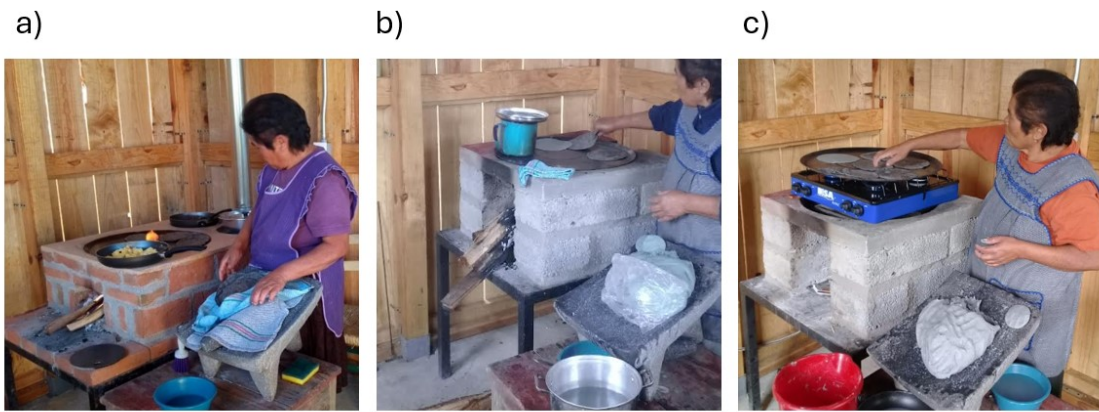
155

156 **5. Stacking options**

157 Table S1. Type of food items cooked with each stove that represent typical consumption patterns
 158 for this region

Cooking task	Stacking Option			
	Patsari-U-Type	Patsari-LPG	LPG-U-Type	Patsari-LPG-U-Type
1. Tortillas	Patsari	Patsari	U-Type	Patsari
2. Fired rice	Patsari	Patsari	U-Type	Patsari
3. Boil beans	U-Type	Patsari	U-Type	U-Type
4. Boil 1L of water	Patsari	LPG	LPG	LPG
5. Reheat	Patsari	LPG	LPG	LPG
6. Fried meals	Patsari	LPG	LPG	LPG

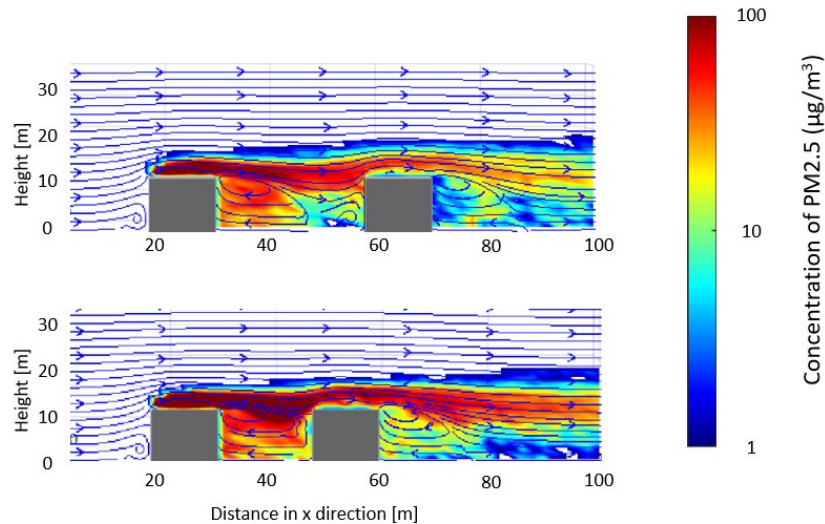
159
 160
 161
 162



163
 164
 165

Figure S7. Testing cook stove type

6. Pollution distribution in a street canyon



167

168 Figure S8. Pollution trapped in the building wakes under (a) interference flow (b) skimming flow

169

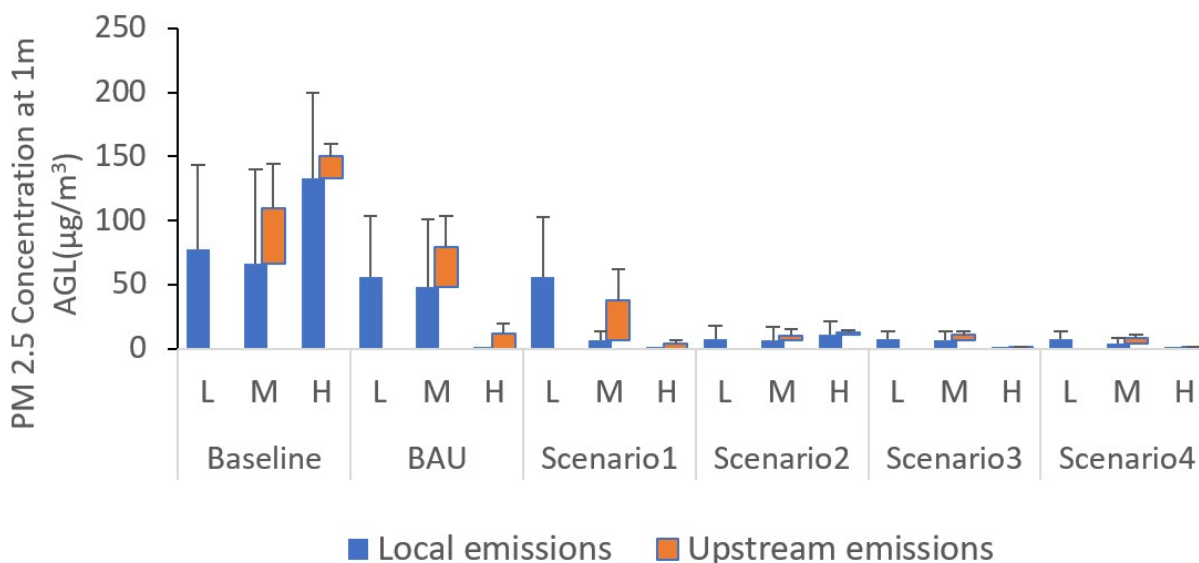
170 Street canyon serves as the basic geometric unit in urban or suburban regions. The configurations
 171 of a village are approximately repetitions of such street canyon units. The aspect ratio, H/W (H is
 172 the height of the building and W is the width between the two buildings) describes the street canyon
 173 features. The flow within a street canyon is determined by the building geometry, street orientation
 174 and wind conditions.

175 As indicated in figure S8, an eddy vortex develops at the building bottom at the windward face,
 176 and on the lee side, there is an eddy entering into the canyon. This is due to the low pressure caused
 177 by the flow separation from the sharp edges on building top and side. Pollutants accumulate with
 178 the backflow downwind of a building, indicating that this recirculation in the building wakes traps
 179 stove emissions for a longer duration. The presence of buildings leads to larger vertical mixing of
 180 the pollutants compared to flat terrain, thus contributing to the near-ground pollution
 181 concentration.

182 If the buildings are far apart, the flow pattern is identical to isolated buildings. When the distance
 183 between the building decrease, the windward side of the downwind building deflects eddies, and
 184 the upstream emission starts to affect the concentrations around the downwind buildings. This
 185 phenomenon is defined as wake interference flow ($2 < W/H < 4$) as figure S8 (a). As the building
 186 wake decreases further, the flow pattern turns to skimming flow ($W/H < 2$) as figure S8(b) shows.
 187 Stable vortices are developed and thus the mixed pollutants are more influential to the downwind
 188 building front side. In addition, the pollutants are difficult to flush out and the particle residence
 189 time is longer since the bulk of the flow does not enter the canyon under this regime. This is one
 190 of the reasons the high-density region is more severely polluted.

191 **7. Implications for indoor impacts**

192 To estimate implications of each scenario on air available for infiltration into indoor environments
 193 average perimeter concentrations of PM_{2.5} at 0.5m away from walls at the height of 1 m around
 194 the exterior walls of each house were computed, which reflects an estimation of air that infiltrates
 195 a home during cooking events. In general, average perimeter concentrations are higher than area
 196 concentrations due to the impacts of the building structure on pollution dispersion, combined with
 197 the lack of emission sources in agricultural areas. Figure S9 shows that perimeter PM_{2.5}
 198 concentrations available for infiltration were higher than WHO interim target 1 for baseline, BAU
 199 and Scenario 1, but meet WHO guideline values for Scenarios 2,3,4.



200

201 Figure S9. Perimeter averaged concentrations for each scenario and each packing density area
 202 (L: Low-packing density area; M: Medium-packing density area; H: High-packing density area)

203

	Baseline			BAU		
	L	M	H	L	M	H
Area	24.92±60.59	54.12±83.31	69.18±83.4	17.94±43.62	38.96±60	0.026±0.03
Perimeter	77.9±65.5	66.5±73.7	133±66.7	56.2±47.1	47.87±53	0.049±0.025
	Scenario 1			Scenario 2		
	L	M	H	L	M	H
Area	17.9±43.62	5.29±8	0.025±0.03	4.08±9.93	8.875±13.67	9.22±11.1
Perimeter	56±47	6.38±7.07	0.049±0.025	7.4±10.74	6.4±10.8	10.68±10.93
	Scenario 3			Scenario 4		
	L	M	H	L	M	H
Area	2.39±5.817	5.19±8	0.025±0.03	2.39±5.81	2.88±5	0.025±0.003
Perimeter	7.48±6.29	6.38±7.07	0.049±0.025	7.49±6.28	3.98±4.42	0.049±0.68

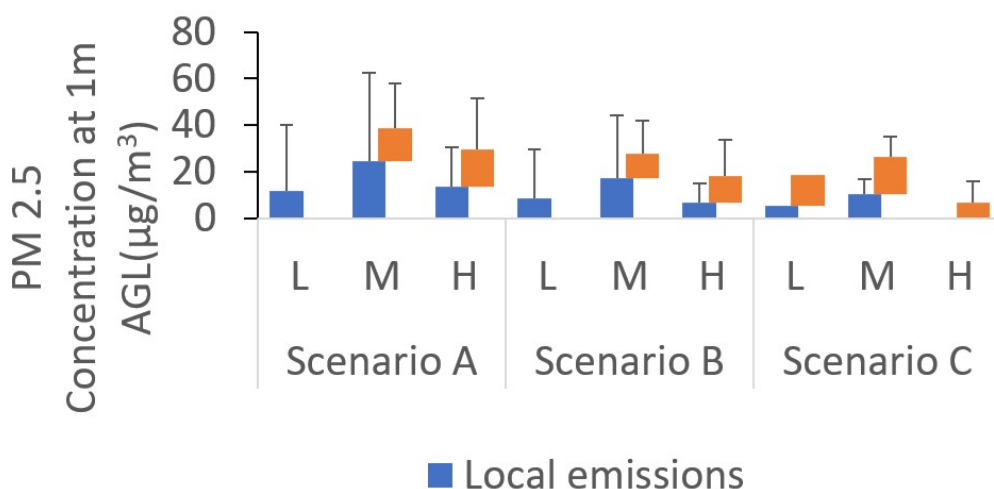
204 Table S2 presents the data table with area concentrations and perimeter concentrations for each
 205 scenario and fraction from upstream, and possibly fraction.

206 Figure S9 above represents an idealized scenario where all homes adopt the interventions.
 207 However, in practice, this is unlikely to occur. A more practical case is simulated in figure 10,
 208 which shows the impacts of 3 different adoption rate schemes in table S3 on average perimeter
 209 concentrations under scenario 4. Here it is assumed that people revert back to use traditional stove
 210 in combination with LPG. The figure demonstrates that even modest decreases in adoption have
 211 substantial impacts on neighborhood pollution concentrations measured at the perimeters of
 212 houses, which highlights the idea of transforming kitchens where the functional utility of the space
 213 is changed, rather than just switching stoves.

214

Packing density	Scenario A	Scenario B	Scenario C
High	LPG 80%; TSF LPG 20%	LPG 90%; TSF LPG 10%	LPG 100%; TSF LPG 0%
Medium	P+G 40%; TSF LPG 60%	P+G 60%; TSF LPG 40%	P+G 80%; TSF LPG 20%
Low	PK+LPG 40%; TSF LPG 60%	PK+LPG 60%; TSF LPG 40%	PK+LPG 80%; TSF LPG 20%

215 Table S3. Adoption rate schemes modeled in QUIC for Scenario 4



216

217 Figure S10. Averaged perimeter concentrations for scenario 4, assuming the adoption rates
 218 shown in table S3

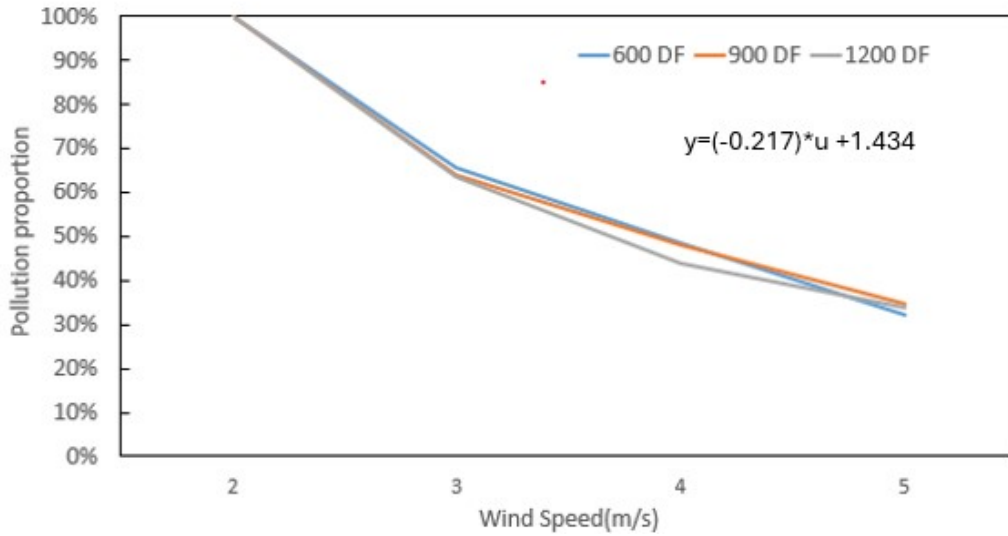
219 (L: Low-packing density area; M: Medium-packing density area; H: High-packing density area)

220

221

222 8. Wind sensitivity analysis

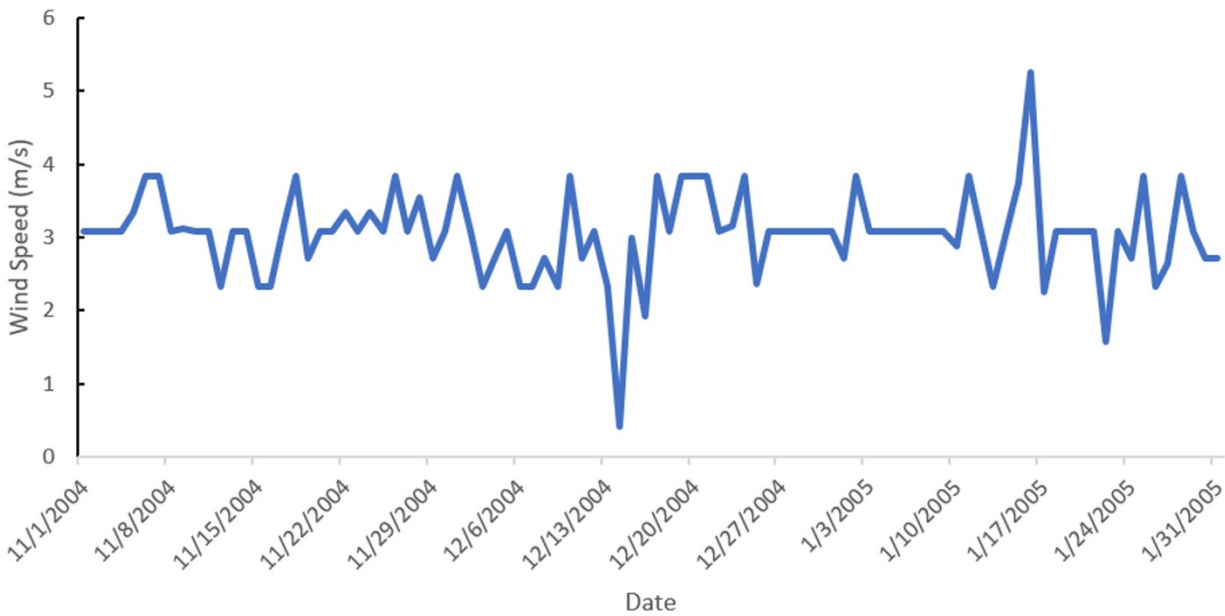
223 The sensitivity of pollution concentrations to wind speed under different density factors is
224 presented in figure S11, indicating that wind speed impact on the pollution concentration is
225 independent of density factor.



226

227

Figure S11. Pollution proportion under different wind speed



228

229

Figure S12. Wind speed during field measurement at village Comachuén

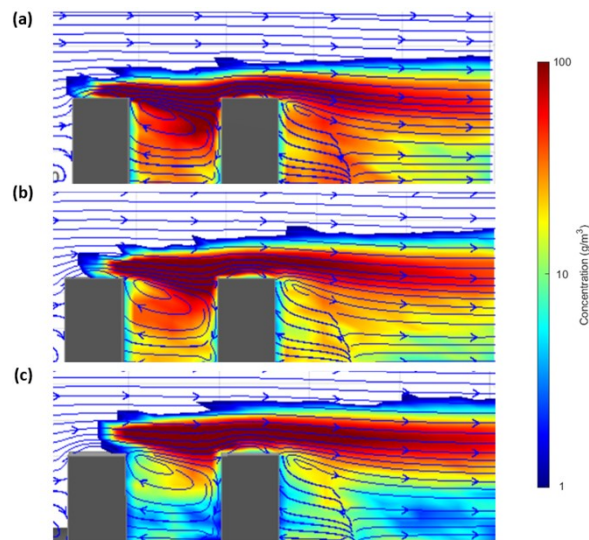
230

231

232

233 9. Chimney height sensitivity analysis

234 To check the sensitivity of pollution dispersion to the height of the chimney above the roof of the
235 building (stack height) at which the pollutant is emitted. Figure S13 (a), (b) and (c) show the
236 concentrations of pollution over the domain when the emission sources are placed at 0.5 m, 1.4 m
237 and 2.2 m height above roof respectively. Increasing stack height shifts $PM_{2.5}$ concentrations
238 further downstream and the region in which the pollution is trapped reduces. However, differences
239 in the average domain concentrations and maximum concentrations due to varied stack heights
240 were small. The majority simulations used a standard stack height of 0.5 m typical for the
241 installation of chimney stoves in the region.



242

243 Figure S13. Pollution accumulation between building wake under different chimney height (a)
244 0.5m; (b) 1.4m; (c) 2.2m

245

246 Michael D. Williams, Michael J. Brown, A. G. (2005). ADAPTATION OF THE QUIC-PLUME MODEL
247 FOR HEAVY GAS DISPERSION AROUND BUILDINGS. *Atmospheric Sciences and Air Quality*
248 *Conferences*.

249 Röckle, R. (1990). *Bestimmung der Strömungsverhältnisse im Bereich komplexer*
250 *Bebauungsstrukturen (Thesis, Dissertation)*.

251 Singh, B., Hansen, B. S., Brown, M. J., & Pardyjak, E. R. (2008). Evaluation of the QUIC-URB fast
252 response urban wind model for a cubical building array and wide building street canyon.
253 *Environmental Fluid Mechanics*, 8(4), 281–312. [https://doi.org/10.1007/s10652-008-](https://doi.org/10.1007/s10652-008-9084-5)
254 9084-5

255 Williams, M., Brown, M., Singh, B., & Boswell, D. (2004). QUIC-PLUME theory guide. *Los Alamos*
256 *National ...*, 1, 1–21.

257 磯部雅晴. (2013). カリフォルニア大学バークレー校(U.C. Berkeley)滞在記. *Near-Source*
258 *Modeling of Transportation Emissions in Built Environments Surrounding Major Arterials*,
259 15(4), 250–260. <https://doi.org/10.11436/mssj.15.250>

260